ROBUST TRACKING IN TWO-DEGREE-OF-FREEDOM CONTROL SYSTEMS: MAGNETIC LEVITATION SYSTEM

P. TEPPA-GARRAN† and M. FAGGIONI‡

† *Departamento de Gestión de Proyectos y Sistemas, Universidad Metropolitana, Caracas, Venezuela*
pteppa@unimet.edu.ve
‡ *Departamento de Energía y Automatización, Universidad Metropolitana, Caracas, Venezuela*
mfaggioni@unimet.edu.ve

***Abstract*— The fundamental result of this work is to provide a connection between an input-output model such as a two-degree-of freedom control system and an equivalent model in the state-space, whose state vector depends exclusively on the measurable information of the original system provided by its outputs. This allows taking advantage of powerful numerical methods to perform controller synthesis and then come back to the two-degree-of-freedom control system for the implementation of the controller. This work focused on state-feedback control laws that ensure robust performance. The effectiveness of the method is validated through the application on the magnetic levitation system.**

***Keywords*— LMI, Magnetic levitation system, Reference following, Robust tracking, Two-degree-of-freedom, 2-DoF.**

I. INTRODUCTION

In a classical feedback control scheme, the control signal is obtained through the difference between the reference and the current output. Since there is only one input to the controller, this classical control structure is also called a one-degree-of-freedom (1-DoF) controller. On the other hand, a controller has 2-DoF, when the reference or the tracking error signals and the plant output, can be processed independently to obtain the control signal. Two fundamental problems arise in the design of control systems. Reference tracking and disturbance attenuation. It is widely known that both problems are produced by the corresponding closed-loop transfer functions (sensitivity and complementary sensitivity) (Safonov *et al.*, 1981). Although, 1-DoF controllers have known structural properties (Davison, 1976), a trade-off must be reached between fast tracking and disturbance attenuation. Whereas disturbance attenuation is exclusively a feedback problem, the tracking problem, is an open-loop property that can be solved by using a suitable precompensator. The advantages of employing a 2-DoF control system are well known: the closed-loop properties can be configured independently of the reference tracking transfer function (Grimble, 1994). This possibility results from the separation between the response to the reference signal and the feedback transfer function. Therefore, the tracking problem is conveniently handled within the 2-DoF control framework.

The objective of this work is to present a simple method to design a 2-DoF controller to solve the robust tracking problem. The main idea of the method is to translate the tracking 2-DoF problem into an auxiliary state-space feedback-control synthesis problem that only uses the measurable information of the plant. The parametric uncertainty of the plant is modeled through a polytope and LMI algorithms (Boyd *et al.*, 1994; Duan and Yu, 2010) are employed to compute control gains assuring both robust tracking and a satisfactory transient response by placing the closed-loop poles in a predefined region of the complex plane. Finally, it is shown how to convert the state-space vector gains into polynomials of the 2-DoF control system for implementing the controller.

The article is outlined as follows. Section 2 depicts the problem formulation. Section 3 provides the main result of the work, where it is stablished a connection between the 2-DoF system and the state-feedback control synthesis problem. Finally, section 4 shows the effectiveness of the method by considering its application to the Magnetic Levitation system.

Notation: Capital bold typeface letters denote matrices and small bold typeface letters denote vectors. $\dot{a} = da/dt$, $\ddot{a}(t) = d^2a/dt^2$, $a^{(i)}(t) = d^ia/dt^i$, $\mathbb{R}$ is the set of real numbers and $A^T = transpose\ of\ A$.

II. PROBLEM FORMULATION

Consider the system described by

$$D(p)y(t) = N(p)u(t) \quad (1)$$

where $y(t) \in \mathbb{R}$ is the plant output and $u(t) \in \mathbb{R}$ is the plant input. $N(p)$ and $D(p)$ are polynomials and p is equal to the time differential operator d/dt or the Laplace complex variable s. Polynomials $D(p)$ and $N(p)$ are written as

$$D(p) = p^n + \sum_{i=0}^{n-1} a_i p^i \, , N(p) = \sum_{i=0}^{m} b_i p^i \quad (2)$$

with $a_i \in \mathbb{R}$ and $b_j \in \mathbb{R}$ for all $i = 0, \ldots, n-1$ and $j = 0, \ldots, m$. The order of the system is defined as the degree of $D(p)$. We also suppose that the system is controllable. In this case, polynomials $D(p)$ and $N(p)$ must be coprime (Antsaklis and Michel, 2006).

In many real-world applications, the uncertainty of the model is reflected in the parameters of the plant equations. In this work, we consider that the coefficients a_i and b_i in (2) may be uncertain and are represented as

$$a_i \in [a_i^-, a_i^+], \, b_i \in [b_i^-, b_i^+] \quad (3)$$

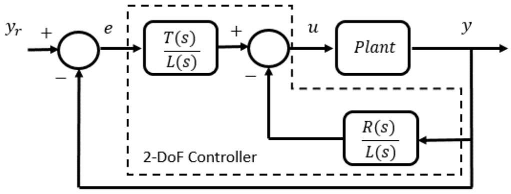

Figure. 1. General 2-DoF control system.

where a_i^-, a_i^+, b_i^- and b_i^+ are known bounds associated with the parameters of the plant model.

A block diagram of a general 2-DoF control system appears in Fig. 1. The 2-DoF controller (Chen, 1999; Landeau and Gianluca, 2006) is given by

$$L(s)u(s) = T(s)e(s) - R(s)y(s) \tag{4}$$

where $e(t) \in \mathbb{R}$ is the tracking error, defined as

$$e(t) = y_r(t) - y(t) \tag{5}$$

with $y_r(t) \in \mathbb{R}$ the input reference and polynomials $L(s), T(s)$ and $R(s)$ are written as

$$\begin{aligned} L(s) &= \textstyle\sum_{i=0}^{n_L} l_i s^i \\ T(s) &= \textstyle\sum_{i=0}^{n_T} t_i s^i \\ R(s) &= \textstyle\sum_{i=0}^{n_R} r_i s^i \end{aligned} \tag{6}$$

Problem 1: Given the plant (1) with parametric uncertainties (3), find polynomials $L(s), T(s)$ and $R(s)$ in (4) to compute the control input $u(t)$ so that the controlled output of the plant $y(t)$ tracks robustly a predefined reference input $y_r(t)$ with zero steady-state error in the 2-DoF control system of Fig. 1.

In the next section, the preceding tracking problem will be solved within a state-space formulation using a LMI approach.

III. PROBLEM SOLUTION

In this section, we consider the problem of designing a 2-DoF controller that provides robust asymptotic tracking of a predefined reference input with zero steady-state error.

A. Plant and equivalent state-space model connection

Associated with system (1), we define the following system:

$$\begin{aligned} \dot{\boldsymbol{x}}(t) &= \boldsymbol{A}\boldsymbol{x}(t) + \boldsymbol{B}u^{(n_c)}(t) \\ &= \begin{bmatrix} \boldsymbol{A_{11}} & \boldsymbol{A_{12}} \\ \boldsymbol{0} & \boldsymbol{A_{22}} \end{bmatrix} x(t) + \begin{bmatrix} \boldsymbol{0} \\ 1 \end{bmatrix} u^{(n_c)}(t), n_c \geq m \\ y(t) &= \boldsymbol{C}\boldsymbol{x}(t) = [1 \quad \boldsymbol{0}]\boldsymbol{x}(t) \end{aligned} \tag{7}$$

The state-vector is selected by considering the measurable information of the plant. That is,

$$\boldsymbol{x} = \left[y, \dots, y^{(n-1)}, u, \dots, u^{(n_c-1)}\right]^T \in \mathbb{R}^N, \quad N = n + n_c \tag{8}$$

The partitioned matrices $\boldsymbol{A_{11}}$, $\boldsymbol{A_{12}}$ and $\boldsymbol{A_{22}}$ are defined as

$$\boldsymbol{A_{11}} = \begin{bmatrix} 0 & 1 & 0 & 0 & \dots & 0 \\ 0 & 0 & 1 & 0 & \dots & 0 \\ \vdots & \vdots & \vdots & \vdots & \ddots & \vdots \\ 0 & 0 & 0 & 0 & \dots & 1 \\ -a_0 & -a_1 & -a_2 & -a_3 & \dots & -a_{n-1} \end{bmatrix}$$

$$\boldsymbol{A_{12}} = \begin{bmatrix} 0 & \dots & 0 & 0 & \dots & 0 \\ 0 & \dots & 0 & 0 & \dots & 0 \\ \vdots & \dots & \vdots & \vdots & \dots & \vdots \\ 0 & \dots & 0 & 0 & \dots & 0 \\ b_0 & \dots & b_m & 0 & \dots & 0 \end{bmatrix}, \boldsymbol{A_{22}} = \begin{bmatrix} 0 & 1 & 0 & \dots & 0 \\ 0 & 0 & 1 & \dots & 0 \\ \vdots & \vdots & \vdots & \ddots & \vdots \\ 0 & 0 & 0 & \dots & 1 \\ 0 & 0 & 0 & \dots & 0 \end{bmatrix}$$

Theorem 1: If System (1) is controllable and all the roots of the polynomial $N(s)$ in (2) are different of zero then system (6) is controllable.

Proof: A simple calculation shows that the transfer function of system (7) can be expressed as

$$\boldsymbol{G(s)} = \frac{\boldsymbol{N(s)}}{\boldsymbol{s^{n_c}D(s)}}$$

If system (1) is controllable, polynomials $\boldsymbol{N(s)}$ and $\boldsymbol{D(s)}$ are coprime. Then, if all the roots of $\boldsymbol{N(s)}$ are different of zero, it follows that $\boldsymbol{N(s)}$ and $\boldsymbol{s^{n_c}D(s)}$ are coprime implying the controllability of system (7) and completing the proof.

B. Uncertainty

For system (1) with parametric uncertainty given as (3). The auxiliary state-space model (7), takes the form of an uncertain polytopic system (Geromel *et al.*, 1991**)** where the state matrix $\boldsymbol{A}$ belongs to an appropiate polytope $\boldsymbol{\mathcal{D}_A}$ with vertices $\boldsymbol{N_A \leq 2^{n+m}}$ that can be characterized as

$$\boldsymbol{A} \in \mathcal{D}_A = \left\{\boldsymbol{A} \in \mathbb{R}^{N \times N}: \boldsymbol{A} = \textstyle\sum_{i=1}^{N_A} \alpha_i \boldsymbol{A_i}, \sum_{i=0}^{N_A} \alpha_i = 1, \alpha_i \geq 0\right\} \tag{9}$$

Here, only the matrix $\boldsymbol{A}$ in (7) is dependent on the interval parametric uncertainty (3).

C. Robust tracking of a step reference

A fundamental result of the control theory is that zero-state tracking errors are achieved by considering in the control policy a suitable model of the dynamic structure of the reference signal (Francis and Wonham, 1976).

Replacing in (5) a step-reference input $y_r(t)$ and using the output equation in (7) gives the time-derivative of the tracking error as

$$\dot{e}(t) = -\boldsymbol{C}\dot{\boldsymbol{x}}(t) \tag{10}$$

Applying now, time-derivative to the state equation in (7) and considering the parametric uncertainty expressed by the polytope (9), yields the augmented step-tracking uncertain system

$$\begin{bmatrix} \dot{e}(t) \\ \ddot{\boldsymbol{x}}(t) \end{bmatrix} = \begin{bmatrix} 0 & -\boldsymbol{C} \\ 0 & A \end{bmatrix} \begin{bmatrix} e(t) \\ \dot{\boldsymbol{x}}(t) \end{bmatrix} + \begin{bmatrix} \boldsymbol{0} \\ \boldsymbol{B} \end{bmatrix} u^{(n_c+1)}(t) \quad \boldsymbol{A} \in \mathcal{D}_A \tag{11}$$

In compact form, (11) can be written as

$$\dot{\boldsymbol{z}}(t) = \boldsymbol{A_{a_i}}\boldsymbol{z}(t) + \boldsymbol{B_a}u_0(t), A_{a_i} = \begin{bmatrix} 0 & -\boldsymbol{C} \\ 0 & \boldsymbol{A_i} \end{bmatrix}, \quad i = 1, \dots, N_A \leq 2^{n+m} \tag{12}$$

where the influence of parametric uncertainty (3) is highlighted through the matrices $\boldsymbol{A_i}$ with index i changing between the different vertices of polytope (9).

For the performance of the closed-loop system, it is employed the state-feedback control law $\boldsymbol{u_0(t)} = \boldsymbol{K_a z(t)}$ in (12), and we consider the placement of the closed-loop poles in a desired LMI region using the following result (Chilali and Gahinet, 1996).

Theorem 2: System (12) where state matrix $\boldsymbol{A}$ belongs to the polytope (9) is stabilizable by a state-feedback control law $\boldsymbol{u_0(t)} = \boldsymbol{K_a z(t)}$ and its closed-loop poles are placed in the LMI region $\boldsymbol{\mathcal{R}(\alpha, \theta, \rho)}$ (see Fig. 2) if and only if there exist a positive definite symmetric matrix $\boldsymbol{S} \in \mathbb{R}^{\boldsymbol{(N+1)x(N+1)}}$ and a matrix $\boldsymbol{R^{1\,x\,(N+1)}}$ such that for the vertices $\boldsymbol{i = 1, \dots, N_A}$ the following LMIs are satisfied

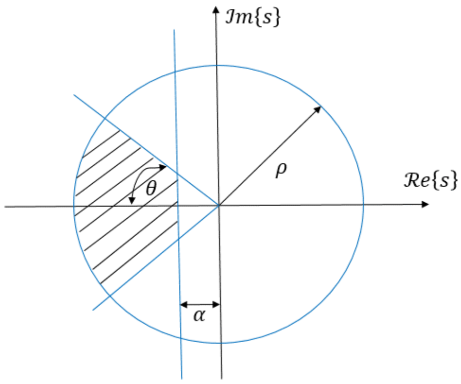

Figure 2. LMI region $\mathcal{R}(\alpha,\theta,\rho)$.

$$\boldsymbol{A}_{a_i}\boldsymbol{S}+\boldsymbol{S}\boldsymbol{A}_{a_i}^{T}+\boldsymbol{B_a}\boldsymbol{R}+\boldsymbol{R}^T\boldsymbol{B_a}^T+2\alpha\boldsymbol{S}<0 \quad (13)$$

$$\begin{bmatrix} -\rho\boldsymbol{S} & \boldsymbol{A}_{a_i}\boldsymbol{S}+\boldsymbol{B_a}\boldsymbol{R} \\ * & -\rho\boldsymbol{S} \end{bmatrix}<0 \quad (14)$$

$$\begin{bmatrix} \sin(\theta)[\Phi] & \cos(\theta)[\Gamma] \\ * & \sin(\theta)[\Phi] \end{bmatrix}<0 \quad (15)$$

$$\Phi = A_{a_i}S + SA_{a_i}^T + B_aR + R^TB_a^T$$
$$\Gamma = A_{a_i}S - SA_{a_i}^T + B_aR - R^TB_a^T$$

The control gain is $\boldsymbol{K_a}=\boldsymbol{R}\boldsymbol{S}^{-1}$.

Although LMI conditions in Theorem 2 are computationally complex to solve. They are easily handled and a numerical solution can be computed using LMI control Toolbox of Matlab (Gahinet *et al*, 1995) or LMITOOL in Scilab (Baudin and Couvert, 2010). Applying Theorem 2 to (12), it places the eigenvalues of closed-loop state matrix $(\boldsymbol{A_a}+\boldsymbol{B_a}\boldsymbol{K_a})$ in the interior of the LMI region of Fig. 2 by means of the control input

$$u_0(t)=\boldsymbol{K_a}\boldsymbol{z}(t) \quad (16)$$

Confining the closed-loop poles to this region ensures a minimum decay rate α, a minimum damping ratio $\xi = cos(\theta)$, and a maximum undamped natural frequency $\omega_d=\rho sin(\theta)$. Expressing gain vector $\boldsymbol{K_a}\in\mathbb{R}^{1\,x\,(N+1)}$ as $\boldsymbol{K_a}=\begin{bmatrix}\underbrace{K_1}_{1x1} & \underbrace{\boldsymbol{K_2}}_{1xN}\end{bmatrix}$ in (16) yields

$$u^{(n_c+1)}(t)=\begin{bmatrix}K_1 & \boldsymbol{K_2}\end{bmatrix}\begin{bmatrix}e(t)\\ \dot{\boldsymbol{x}}(t)\end{bmatrix} \quad (17)$$

Next, it is found the relation between the gains K_1 and $\boldsymbol{K_2}$ in (17) with the polynomials $L(s),T(s)$ and $R(s)$ of the 2-DoF controller in (4). After performing time-integration in (17) and using the state-vector $\boldsymbol{x}(t)$ from (7), the control signal $u^{(n_c)}(t)$ can be written as

$$u^{(n_c)}(t)=K_1\int_0^t e(\tau)\,d\tau+\boldsymbol{K_2}\begin{bmatrix}y(t)\\ \vdots \\ y^{(n-1)}(t)\\ u(t)\\ \vdots\\ u^{(n_c-1)}(t)\end{bmatrix}$$

Partitioning vector $\boldsymbol{K_2}$ as $[\boldsymbol{K_{2y}} \quad \boldsymbol{K_{2u}}]$ gives

$$u^{(n_c)}(t)=K_1\int_0^t e(\tau)\,d\tau+\begin{bmatrix}\underbrace{r_0 \quad \cdots \quad r_{n-1}}_{K_{2y}}\end{bmatrix}\begin{bmatrix}y(t)\\ \vdots\\ y^{(n-1)}(t)\end{bmatrix} + \begin{bmatrix}\underbrace{l_0 \quad \cdots \quad l_{n_c-1}}_{K_{2u}}\end{bmatrix}\begin{bmatrix}u(t)\\ \vdots\\ u^{(n_c-1)}(t)\end{bmatrix}$$

Table 1. Algorithm for computing polynomials R, L and $T$of the 2-DoF control system.

Input	Plant polynomials $N(p)$ and $D(p)$ in (2) Plant parametric uncertainty bounds $a_i^-, a_i^+, b_i^-, b_i^+$ in (3)
Step 1	Define the augmented vector $\boldsymbol{x}(t)$ used in (7)
Step 2	Compute matrices $\boldsymbol{A}_{a_i}$ for $i=1,..,N_A$ and matrix $\boldsymbol{B_a}$ in (12)
Step 3	Define the LMI region $\mathcal{R}(\alpha,\theta,\rho)$
Step 4	Solve for gain $\boldsymbol{K_a}$ the Theorem 2
Step 5	Using the components of vector $\boldsymbol{K_a}$, compute polynomials R, L and T in (18)
Output	Polynomials $R(s), L(s)$ and T(s) in (4)

Taking the Laplace transform of the above equation yields (4), where the polynomials $L(s), T(s)$ and $R(s)$ are identified as

$$L(s)=-l_0-l_1s-\cdots-l_{n_c-1}s^{n_c-1}+s^{n_c}$$
$$T(s)=K_1/s \quad (18)$$
$$R(s)=-r_0-r_1s-\cdots-r_{n-1}s^{n-1}$$

These results are summarized in Theorem 3 and for ease of reference; they are outlined in the algorithm of Table 1.

Theorem 3: Given the plant (1) with parametric uncertainties (3), then control signal $u(t)$ in (4), for the 2-DoF control system of Fig. 1, can be computed through the polynomials (18) so that the controlled output of the plant $y(t)$ tracks robustly and asymptotically any step-reference input $y_r(t)$ placing the poles of the closed-loop system (12) in the LMI region of Fig. 2.

The internal model principle is easily extended to other persistent reference inputs (ramps, sinusoids, etc.) by following the same general procedure outlined for the step input. In the same way, other robust performance criteria can be addressed by employing similar ideas to those used for closed-loop pole placement. For instance, the criteria $\mathcal{H}_2$ and $\mathcal{H}_\infty$ (Teppa-Garran, 2008).

IV. NUMERICAL VALIDATION

In this section, the proposed method is applied to the magnetic levitation system (maglev) system. The maglev is a popular plant to test control methods and has also received great interest because of its practical importance in many engineering systems, such as: high speed maglev passenger trains, frictionless bearings, levitation of wind tunnel models, vibration isolation of sensitive machinery, levitation of molten metal in induction furnaces, and levitation of metal slabs during manufacturing (Muthairi and Zribi, 2004). The control objective for the maglev system is to regulate the position of a steel ball by controlling the current passing through an electromagnet. Several controlling policies have been proposed, among them, one can mention: constrained control (Huba and Kamensky, 2005), state-space control (Lee *et al.*, 2007), polynomial control (Gazdos *et al.*, 2009), sliding-mode control (Shieh *et al.*, 2010), PID control (Hypiusova and Kozakova, 2017), fuzzy control (Farana *et al.*, 2015), adaptive control (Bidikli, 2020) and model predictive control

Figure 3. Maglev system.

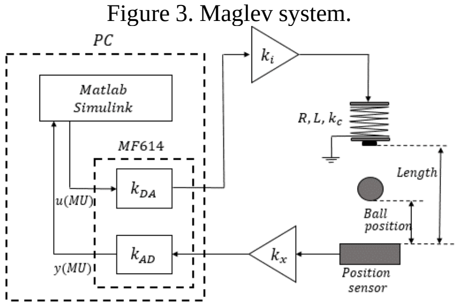

Figure 4. Schematic diagram of the maglev system.

Table 2. Physical parameters and values of the maglev system.

Variables/ parameters	Description	Value and unit
k_{AD}	A/D converter gain	$0.2\ MU^a/V$
k_{DA}	D/A converter gain	$20\ V/MU^a$
k_{fv}	Damping constant	$0.02\ Ns/m$
k_x	Position sensor gain	$821\ V/m$
k_i	Power amplifier gain	$0.3\ A/V$
k_c	Coil constant	$1.8\text{x}10^{-6}\ Nm^2/A^2$
m_k	Ball mass	$8.27\text{x}10^{-3}\ kg$
x_0	Coil offset	$7.6\text{x}10^{-3}\ m$
g	Gravity constant	$9.81\ m/s^2$
y_0	Position sensor offset	$0.0183\ V$
$y(t)$	Ball position	MU^a
$u(t)$	Input signal	MU^a

[a]Voltage converted by the data acquisition card and scaled to ± 1 machine unit (MU).

(Chalupa *et al.*, 2017; Rusar *et al.*, 2017; Wang *et al.*, 2021).

A. Magnetic levitation system

The maglev system CE 152 (Fig. 3) consists of a coil levitating a steel ball in the magnetic field. With position sensed by an inductive linear sensor connected to an A/D converter. The coil is driven by a power amplifier linked to a D/A converter. The plant is connected to a computer, via the universal data acquisition card MF614 and is controlling by employing the Matlab/Simulink environment. Detailed description of the apparatus can be found in Humosoft (2002). A state space model of the system with x_1 corresponding to the ball position and x_2 describing its speed is derived in Humosoft (2002).

$$\dot{x}_1 = x_2$$
$$\dot{x}_2 = \frac{k_{fv}}{k_{AD}k_x}x_2 + \frac{k_{AD}k_x k_{DA}^2 k_i^2 u^2 k_c}{m_k\left(\frac{x_1 - k_{AD}y_0}{k_{AD}k_x} - x_0\right)} - k_{AD}k_x g. \quad (19)$$

where $u(t)$ is the control input, proportional to the voltage from D/A converter. Other symbols used in (19) and their actual values are defined in Table 2 and a schematic diagram showing the simplified internal connections of the maglev appears in Fig. 4.

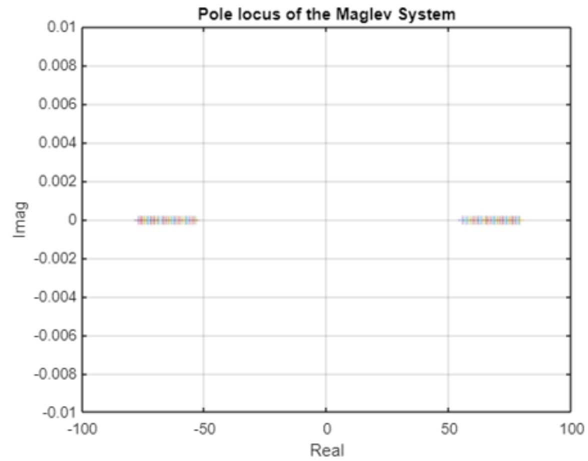

Figure 5. Poles of the Maglev linear model when parameters are varying in interval (22).

Equation (19) is linearized in the operating point (u_{eq}, y_{eq}). The nominal operation is chosen with the ball levitating in the middle of the space. Two other operations points are considered, which differ from the nominal operation a distance of $\pm 30\%$. From the resultant linear state space description is computed the second order differential equation

$$\ddot{y}(t) - \frac{k_{fv}}{m_k}\dot{y}(t) - \frac{2g}{k_{DA}k_i u_{eq}\sqrt{\frac{k_c}{m_k g}}}y(t) = \frac{2k_{AD}k_x g}{u_{eq}}u(t) \quad (20)$$

where $y(t)$ is the ball position. Equation (20) is used exclusively for controller design. The uncertain model that describes the operation of the maglev system throughout the entire operating range is

$$\ddot{y}(t) - 2.418\dot{y}(t) - a_0 y(t) = b_0 u(t) \quad (21)$$

With the uncertain parameters varying within the intervals

$$a_0 \in [a_0^-, a_0^+] = [2963, 6134]$$
$$b_0 \in [b_0^-, b_0^+] = [13638, 28231] \quad (22)$$

Figure 5 shows the poles for different values of parameter a_0 changing in the interior of interval (22). It can be seen that the system has one stable pole and one unstable pole located symmetrically on the real axis.

B. Polytopic representation of the maglev system

Defining the state vector as $\boldsymbol{x}(t) = [y(t) \quad \dot{y}(t) \quad u(t) \quad \dot{u}(t)]^T$ in (7), the maglev system model (21) takes the form

$$\dot{x}(t) = \begin{bmatrix} 0 & 1 & 0 & 0 \\ a_0 & 2.418 & b_0 & 0 \\ 0 & 0 & 0 & 1 \\ 0 & 0 & 0 & 0 \end{bmatrix} x(t) + \begin{bmatrix} 0 \\ 0 \\ 0 \\ 1 \end{bmatrix} \ddot{u}(t)$$
$$y(t) = [1 \quad 0 \quad 0 \quad 0]x(t) \quad (23)$$

With parameters a_0 and b_0 varying within the intervals given by (22) and in this way producing that the steel ball changes its position in the magnetic field from -30% to $+30\%$ of the nominal operation point. Using the extreme values in (22) allows obtaining the four vertices in (24) for the polytope characterized by the state matrices

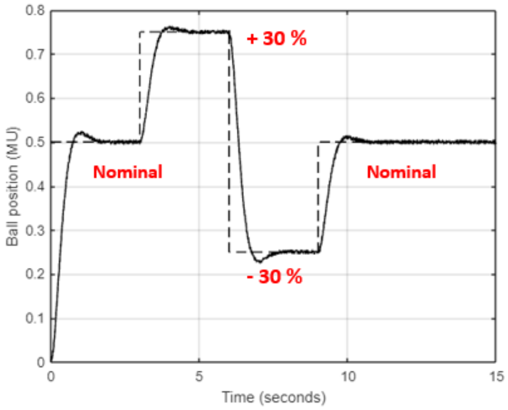

Figure 6. Ball position response for the maglev system.

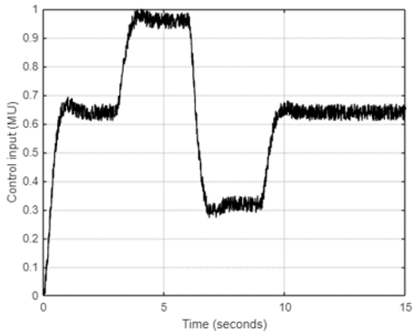

Figure 7. Control signal for the maglev system.

$$\boldsymbol{A_1} = \begin{bmatrix} 0 & 1 & 0 & 0 \\ 2963 & 2.418 & 13638 & 0 \\ 0 & 0 & 0 & 1 \\ 0 & 0 & 0 & 0 \end{bmatrix} \quad (24)$$
$$\boldsymbol{A_2} = \begin{bmatrix} 0 & 1 & 0 & 0 \\ 2963 & 2.418 & 28231 & 0 \\ 0 & 0 & 0 & 1 \\ 0 & 0 & 0 & 0 \end{bmatrix}$$
$$\boldsymbol{A_3} = \begin{bmatrix} 0 & 1 & 0 & 0 \\ 6134 & 2.418 & 13638 & 0 \\ 0 & 0 & 0 & 1 \\ 0 & 0 & 0 & 0 \end{bmatrix}$$
$$\boldsymbol{A_4} = \begin{bmatrix} 0 & 1 & 0 & 0 \\ 6134 & 2.418 & 28231 & 0 \\ 0 & 0 & 0 & 1 \\ 0 & 0 & 0 & 0 \end{bmatrix}$$

C. DoF design for tracking a step reference input

For a step reference input, the augmented step-tracking uncertain system (12) has matrices

$$\boldsymbol{A_{a_1}} = \begin{bmatrix} 0 & -1 & 0 & 0 & 0 \\ 0 & 0 & 1 & 0 & 0 \\ 0 & 2963 & 2.418 & 13638 & 0 \\ 0 & 0 & 0 & 0 & 1 \\ 0 & 0 & 0 & 0 & 0 \end{bmatrix} \quad (25)$$
$$\boldsymbol{A_{a_2}} = \begin{bmatrix} 0 & -1 & 0 & 0 & 0 \\ 0 & 0 & 1 & 0 & 0 \\ 0 & 2963 & 2.418 & 28231 & 0 \\ 0 & 0 & 0 & 0 & 1 \\ 0 & 0 & 0 & 0 & 0 \end{bmatrix}$$
$$\boldsymbol{A_{a_3}} = \begin{bmatrix} 0 & -1 & 0 & 0 & 0 \\ 0 & 0 & 1 & 0 & 0 \\ 0 & 6134 & 2.418 & 13638 & 0 \\ 0 & 0 & 0 & 0 & 1 \\ 0 & 0 & 0 & 0 & 0 \end{bmatrix}$$
$$\boldsymbol{A_{a_4}} = \begin{bmatrix} 0 & -1 & 0 & 0 & 0 \\ 0 & 0 & 1 & 0 & 0 \\ 0 & 6134 & 2.418 & 28231 & 0 \\ 0 & 0 & 0 & 0 & 1 \\ 0 & 0 & 0 & 0 & 0 \end{bmatrix}$$
$$B_a = [0 \quad 0 \quad 0 \quad 0 \quad 1]^T$$

Using (25) and LMI region $\mathcal{R}(0.5, \pi/4, 1)$ in Theorem 2 yields gain vector $\boldsymbol{K_a}$

$$\boldsymbol{K_a} = [\underbrace{0.0018}_{K_1} \quad \underbrace{-890.6}_{r_0} \quad \underbrace{-4.0}_{r_1} \quad \underbrace{-4098.6}_{l_0} \quad \underbrace{-15.7}_{l_1}]$$

From vector $\boldsymbol{K_a}$, it is possible to recovery the polynomials $L(s)$, $T(s)$ and $R(s)$ for the 2-DoF control structure as

$$L(s) = -l_0 + -l_1 s = 4098.6 + 15.7s$$
$$T(s) = K_1/s = 0.0018/s$$
$$R(s) = -r_0 - r_1 s = 890.6 + 4s$$

The results appear in Fig. 6 and 7 where the controlled position of the steel ball and the control signal are scaled to fit the range between 0 and 1. The position of the steel ball is varying from $-30\ \%$ to $+30\ \%$ of the nominal operation.

Figure 8 shows the effect of varying parameter $\boldsymbol{\alpha}$ in LMI region $\boldsymbol{\mathcal{R}}(\boldsymbol{\alpha}, \boldsymbol{\pi/4}, \mathbf{1})$ (Fig. 2) on the transient response of the maglev system and Fig. 9 when the angle $\boldsymbol{\theta}$ changes in $\boldsymbol{\mathcal{R}}(\mathbf{0.3}, \boldsymbol{\theta}, \mathbf{1})$.

V. CONCLUSIONS

The proposed method to achieve robust tracking of the position of the maglev system had a satisfactory performance. The methodology can be extended to other reference signals and other robustness criteria could be incorporated, such as $\mathcal{H}_2$ or $\mathcal{H}_\infty$. Currently work focuses on adapting the method to design 2-DoF controllers to MIMO systems.

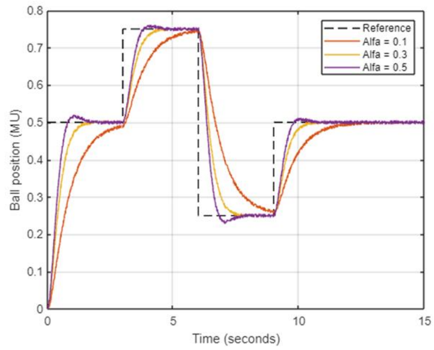

Figure 8. Ball position for three different values of $\boldsymbol{\alpha}$ in $\mathcal{R}(\alpha, \pi/4, 1)$.

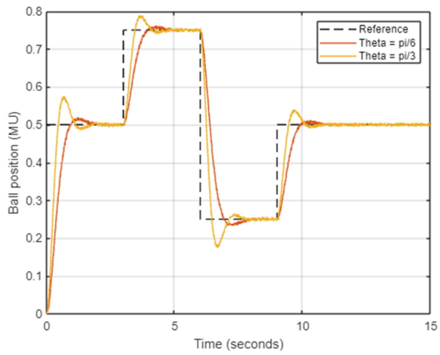

Figure 9. Ball position for two different values of θ in $\mathcal{R}(0.5, \theta, 1)$.

ACKNOWLEDGMENTS

The authors are grateful for the support provided by the Research Program of the Metropolitan University in Caracas, Venezuela through project number PI-A-13-21-22.

REFERENCES

Antsaklis, P. and Michel, A. (2006) *Linear Systems*. Boston, USA, Birkhauser.

Baudin, M. and Couvert, V. (2010). *Optimisation in Scilab*. Consortium Scilab. Francia.

Bidikli, B. (2020) An observer-based adaptive control design for the maglev system. *Transactions of the Institute of Measurement and Control*. **42**, 2771-2786.

Boyd, S., El Ghaoui, L., Feron, E. and Balakrishnan, V. (1994) *Linear matrix inequalities in system and control theory*. Society for industrial and applied mathematics.

Chalupa, P., Novak, J. and Maly, M. (2017) Modelling and model predictive control of magnetic laboratory plant. *Proc of 31st European Conference on Modelling and Simulation*. Hungary, 367-373.

Chen, C. (1999) *Linear System: Theory and Design*. Oxford University Press.

Chilali, M., and Gahinet, P. (1996) $\mathcal{H}_\infty$ design with pole placement constraints: an lmi approach. *IEEE Transactions on automatic control*. **41**, 358-367.

Davison, E. (1976) The robust control of a servomechanism problem for linear-time-invariant multivariable systems. *IEEE Transactions on Automatic Control*. **21,** 25-34.

Duan, G.R. and Yu, H.H. (2013) *LMIs in control systems: analysis, design and applications*. CRC press.

Farana, R., Walek, B., Janosek, M. and Zacek, J. (2015) Advantages of fuzzy control application in fast and sensitive technological processes. *Int. J. Electr. Comput. Eng*. **9**, 1270-1274.

Francis, B.A. and Wonham, W.M. (1976) The internal model principle of control theory. *Automatica*. **12**, 457-465.

Gahinet, P., Nemirovski, A., Laub, A. and Chilali, M. (1995) *LMI Control Toolbox User´s Guide*. The Mathwork Partner Series.

Gazdos, F., Dostal, P. and Pelikan, R. (2009) Polynomial approach to control system design for a magnetic levitation system. *Cybern. Lett*. **7**, 1-19.

Geromel, J.C., Peres, P.L. and Bernussou, J. (1991) On a convex parameter space method for linear control design of uncertain systems. *SIAM J. on Cont. Opt.* **29**, 381-402.

Grimble, M. (1994) *Robust industrial control. Optimal design approach for polynomial systems*. Prentice-Hall International, New Jersey, USA.

Huba, M. and Kamensky, M. (2005) Constrained magnetic levitation control. *IFAC Proc*. **308**, 901-906.

Humosoft (2002) CE152 *Magnetic Levitation Model-educational manual*, Prague Humosoft s.r.o.

Hypiusova, M. and Kozakova, A. (2017) Robust PID controller design for the magnetic levitation system: Frequency domain approach. *Proc. of 21st International Conference on Process Control*. Slovakia, 274-279.

Landeau, I. and Gianluca, Z. (2006) *Digital Control Systems: Design, Identification and Implementation*. Springer-Verlag, London, UK.

Lee, T., Su, J. and Yu, K. (2007) Implementation of the state-space feedback control scheme for a magnetic levitation system. *Proc 2nd IEEE Conference on Industrial Electronics and Applications*. China, 548-553.

Muthairi, N. and Zribi, M. (2004) Sliding mode control of a magnetic levitation system. *Mathematical problems in Engineering*. 93-107.

Rusar, L., Krhovjak, A. and Bobal, V. (2017) Predictive control of the magnetic levitation model. *Proc. of 21st International Conference on Process Control*. Slovakia, 345-350.

Safonov, M., Laub, A. and Hartmann, G. (1981) Feedback properties of multivariable systems: the role and use of the return difference matrix. *IEEE Transactions on Automatic Control*. **40**, 841-852.

Shieh, H., Siao, J. and Liu, Y. (2010) A robust optimal sliding-mode control approach for magnetic levitation systems. *Asian Journal of Control*. **12**, 480-487.

Teppa-Garran, P. (2008) Robust control of a linear parameter varying system: A LMI approach. *Revista de la Facultad de Ingeniería Universidad Central de Venezuela*. **23**, 5-17.

Wang, J., Chen, L. and Xu, Q. (2021) Disturbance estimation based robust model-predictive position tracking control for Magnetic Levitation System. *IEEE/ASME Transactions on Mechatronics*. **27**, 81-92.

Received: July 7, 2022
Sent to Subject Editor: August 29, 2022
Accepted: December 16, 2022
Recommended by Subject Editor Diego Feroldi